



Dynamics of self-pulsing semiconductor lasers with optical feedback

O. Carroll, Y. Tanguy, J. Houlihan^{*}, G. Huyet

Physics Department, National University of Ireland, University of College Cork, Ireland

Received 25 February 2004; received in revised form 2 June 2004; accepted 3 June 2004

Abstract

We analyse the dynamics of a self-pulsating semiconductor laser with optical feedback. Without re-injection of light the laser displays periodic oscillations. At very weak feedback levels we observe an amplitude instability whose frequency increases with the feedback level until the laser enters the low frequency fluctuation regime commonly observed in cw lasers with optical feedback. We show that such behaviour can be observed within the framework of the Lang–Kobayashi equations for self-pulsating semiconductor lasers.

© 2004 Elsevier B.V. All rights reserved.

PACS: 42.55.P; 82.40.Bj

Keywords: Semiconductor; Laser; Dynamics; Relaxation oscillation; Nonlinear; External cavity; Feedback

1. Introduction

Instabilities induced by optical feedback have been the subject of numerous studies. In particular, the re-injection of light into a semiconductor diode can generate periodic and aperiodic fluctuations at a frequency related to the relaxation oscillations and external cavity frequencies [1]. The amplitude of these oscillations increases with the

feedback level and secondary instabilities occur. In general these instabilities are associated with the large line-width enhancement factor characteristic of semiconductor laser. As a result, pulsation of the laser intensity induces a strong frequency modulation which couples all of the external cavity modes, that may merge and generate a single chaotic attractor characterised by the appearance of low frequency fluctuations (LFFs) [2–5]. The aim of this paper is to analyse the appearance of these instabilities in self-pulsating semiconductor lasers. These devices, where unpumped regions act as saturable absorbers [6–8] and the relaxation

^{*} Corresponding author. Tel.: +353214902053; fax: +353214276949.

E-mail address: houlihan@phys.ucc.ie (J. Houlihan).

oscillations become undamped, are commonly used in various applications such as in compact disk players. It has been observed that these devices have poor coherence properties and therefore have a low sensitivity to back reflections [9]. However, recently a theoretical analysis showed that the presence of a saturable absorber can also increase the sensitivity to optical feedback [10]. Here, we experimentally analyse the fast dynamics of a self-pulsating semiconductor laser which displays periodic oscillations at a few GHz. As the optical feedback was increased, we observed the appearance of an amplitude instability whose frequency increased with feedback level until the device entered the LFF regime. Such dynamics are analysed in the framework of the Lang–Kobayashi equations [11] for self-pulsating semiconductor lasers where the amplitude instability is associated with external cavity mode hopping.

2. Experiment

The self-pulsing laser consists of a single transverse mode unstable resonator with saturable absorber as shown on Fig. 1 emitting at 980 nm. The unpumped region just before the laser's cleaved facet acts as a saturable absorber leading to self-pulsation of the laser intensity. In the results presented in this paper, the device was operated with periodic, ≈ 200 ns square pulses with a duty cycle of 0.2% provided by an Avtech power supply (AVI-V-HV2-B) to avoid the appearance

of thermal effects which will alter the spatial profile of the device. In the continuous wave regime, the onset of thermal lensing causes a weak modulation in the amplitude of the pulses over times-scales of around 1 μ s. In the pulsed regime, the periodic oscillations existed over a wide range of voltage currents, a typical example of which is shown on Fig. 2(top). The frequency of these oscillations varied with injection voltage as shown on the same figure. The drive voltage is directly proportional to the drive current due to the presence of an impedance matching resistance in the biasing circuit and we observed that the self-pulsing frequency squared was proportional to the injection current as for the damped relaxation oscillations of cw semiconductor lasers. The beam characteristics of the laser were examined within this range of operation and confirmed single spatial mode oscillation. In particular, we measured the laser intensity in various point of the laser beam using two 30 ps rise-time detectors (Newport D-30 FC) and a 6 GHz real-time oscilloscope (LeCroy Wavemaster 8600) and observed perfect spatial correlation of the self-pulsation. Throughout the paper, we ascertain the effect of the instability on the spatial coherence of the device and note that the device remained single transverse mode for all the measurements presented in this paper.

To examine the effect of coherent optical feedback on the dynamics of the self-pulsing laser an external cavity was constructed as shown on Fig. 3. A cylindrical lens had to be used to ensure full spatial mode overlap between the laser and external cavity

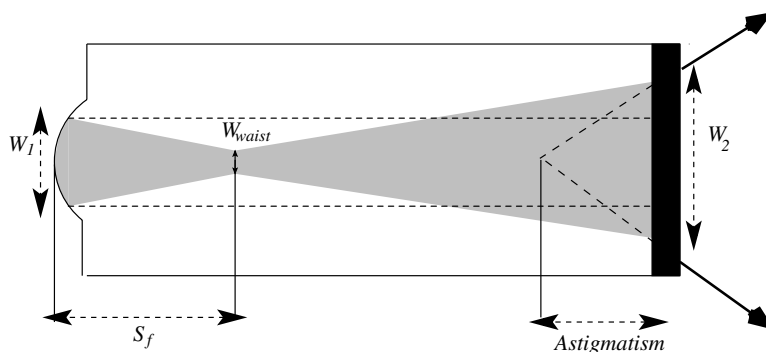


Fig. 1. A schematic of the self-pulsing laser's optical cavity geometry and injection contact. The radius of the curved mirror is 300 μ m and the length of the optical cavity is 1 mm.

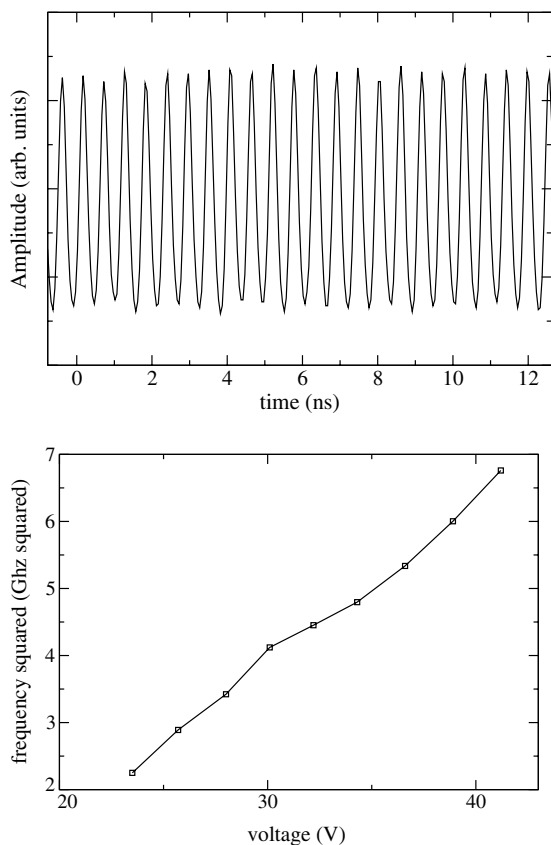


Fig. 2. (top) A typical time-trace of the output power of the laser in self-pulsing mode. (bottom) Self-pulsing frequency squared vs. voltage for a 50 Ω impedance matched laser. The linear behaviour suggests a relaxation oscillation linked process.

fields as the unstable resonator leads to an astigmatic output from the laser. A beam splitter was positioned in the external cavity in order to couple the output power to a detection branch. An optical isolator prevented back reflection from the detection branch into the laser. The light was coupled to a multi-mode fiber before detection on a 30 ps rise-time detector. The signal was analysed by the 6 GHz real time oscilloscope and/or 26 GHz radio frequency analyser (Rohde and Schwarz, FSEM 20).

For external cavity lengths shorter than 10 cm, the relaxation oscillation frequency locked to the external cavity frequencies and chaotic dynamics was observed as the feedback level was increased. This behaviour is similar to that observed with cw semiconductor lasers. However, for longer

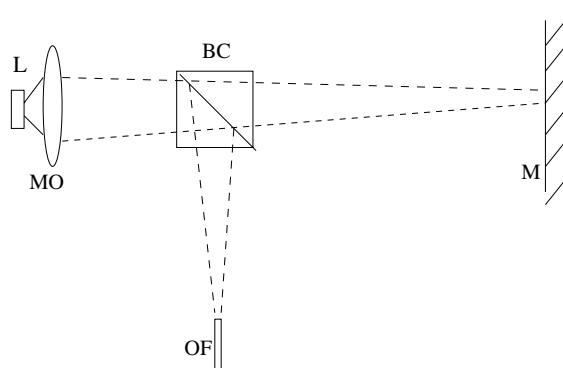


Fig. 3. Schematic of the experimental setup used to analyse the effect of optical feedback on the self-pulsing laser (L) using a microscope objective (MO), a beam splitter cube (BC) and an external mirror (M). An optical isolator (not shown) is used before the optical fiber (OF) to remove any perturbations from the diagnostics. A cylindrical lens (not shown) is also included in the external cavity to ensure spatial mode matching.

external cavity lengths of about 30 cm we observe a new type of instability at weak values of the feedback level, ≈ -28 dB. For this feedback level, we observed the appearance of events where the amplitude of the pulses abruptly decreases to the average power of the compound laser system as shown on Figs. 4 and 5. To further analyse these events, we measured the Hilbert phase [12] and noted that the instantaneous frequency of the self-pulsation remained unchanged when the intensity of the pulses dropped. This indicates that these events are associated with an amplitude instability. As the feedback level was increased, the mean frequency of this amplitude instability increased although the time between consecutive events was not constant. For further increases in the feedback level, the amplitude variation of the pulses increased to RMS values of around 30% of the solitary laser, as the feedback varies up to ≈ -15 dB. In this regime, several external cavity round-trip frequencies can be observed in the radio-frequency power spectrum as shown on Fig. 6.

When the feedback level was further increased to -13 dB, LFFs, similar to those observed in cw semiconductor lasers, appeared in the time averaged output of the compound laser as shown on Fig. 7. These oscillations persisted for much longer pulsewidths, however a low frequency envelope

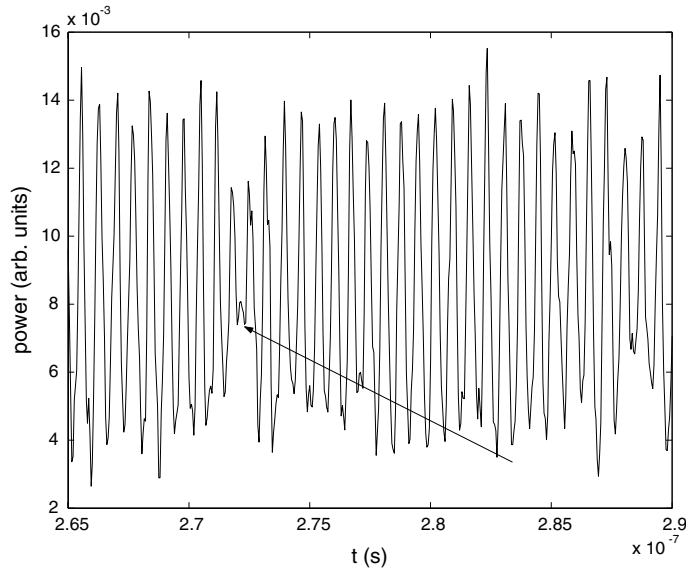


Fig. 4. An example of an interruption in the self-pulsing output of the compound laser system at a feedback level of -28 dB.

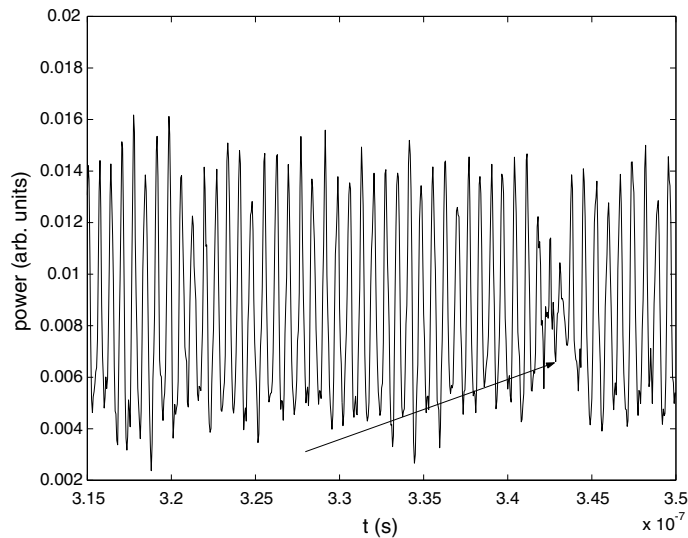


Fig. 5. A second example of an interruption in the self-pulsing output of the compound laser system at a feedback level of -28 dB.

also appears due to thermal transverse mode switching which we will not discuss here. We compared the threshold for the LFF regime with that of a cw laser. The cw device was similar to that described above but designed without an absorbing region and did not display oscillations without optical feedback. In this cw laser, LFF were observed

at -18.5 dB, a value which is much lower than that measured with the self-pulsing laser (-13 dB). It is worthwhile to notice that self-pulsating lasers have previously been found less sensitive to optical feedback [9], this reduction in sensitivity being attributed to the loss in coherence of the laser between pulses because the power goes to zero. In-

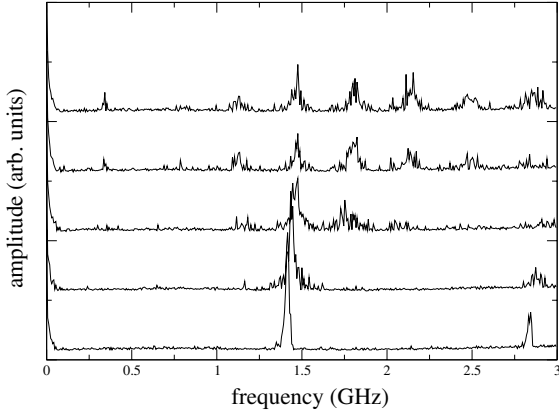


Fig. 6. Power spectra of the compound laser at feedback levels ranging from -25 to -15 dB.

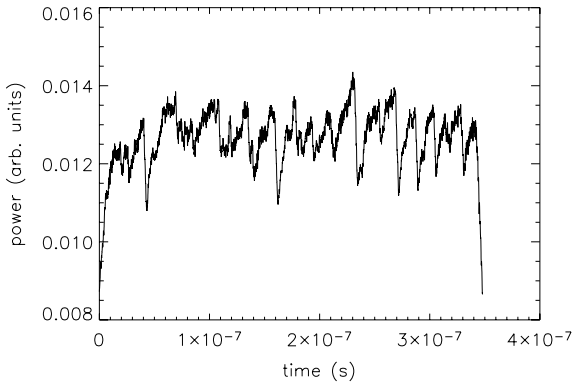


Fig. 7. A typical low bandwidth filtered time trace of the compound laser signal indicating the presence of LFFs. The feedback level is -9 dB.

deed, our laser is also less sensitive to optical feedback than a similar cw semiconductor laser although the power is not low between consecutive oscillations. This indicates that the reduced sensitivity to optical feedback is not only associated with the loss of coherence between consecutive pulses but rather with the self sustained relaxation oscillations.

3. Theory

As for continuous wave semiconductor lasers with optical feedback, it is worthwhile to numeri-

cally investigate these phenomena within the framework of the Lang–Kobayashi equations as this provides access to the temporal evolution of the phase [11]. For example, further understanding of the relevant dynamics can be obtained by projecting the numerically obtained trajectory onto the plane defined by the phase difference $\eta(t) = \varphi(t) - \varphi(t - \tau)$, and either the laser intensity or the carrier density. In the case of cw lasers, it was found that, for some parameter regimes, the phase dynamics can be described in terms of a potential whose minima correspond to stable external cavity modes [13]. Additionally, these modes can be destabilised by a Hopf bifurcation whose frequency is associated with the solitary laser’s relaxation oscillations [14–18], and thus a limit cycle is created near each external cavity mode. When the feedback level is further increased, these limit cycles become chaotic and merge to generate a low frequency attractor [2,3]. For self-pulsating semiconductor lasers, the effect of the absorbing region can be described by the inclusion of an additional carrier density [7,8] and the resulting equations read:

$$\begin{aligned} \frac{\partial E}{\partial t} &= \frac{1}{\tau_e} (E + i\alpha E)(N + n - 1) + \gamma e^{i\phi} E(t - \tau), \\ \frac{\partial N}{\partial t} &= -\frac{1}{\tau_N} (N - J + N|E|^2), \\ \frac{\partial n}{\partial t} &= -\frac{1}{\tau_n} (n + A + \beta N|E|^2), \end{aligned} \quad (1)$$

where E, N and n are the electric field and carrier densities in the pumped and unpumped region, respectively, τ_e, τ_N and τ_n are the field and carrier density decay rates for each of the different carrier

Table 1
Parameter values for Lang–Kobayashi based simulation

Parameter	Value
Field decay time (τ_e)	1
Carrier decay time (τ_N)	20
Carrier decay rate (τ_n)	20
External cavity round-trip phase (ϕ)	0
External cavity round-trip time (τ)	1500
Pump current (J)	3.72
Saturable absorption (A)	2
Saturation intensity ratio (β)	3.2

densities. Also, α is the phase-amplitude coupling of the medium, γ is the feedback level, ϕ is the external cavity round-trip phase, τ is the external

cavity round-trip time, J is the pump current, normalised to have $J=0$ at transparency and $J=1$ corresponding to the solitary laser threshold.

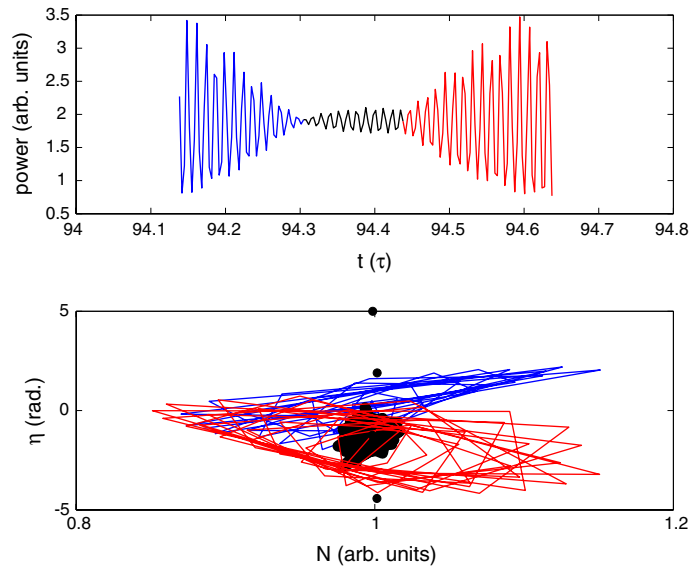


Fig. 8. Simulated optical power (top) and $(\eta(t) = \varphi(t) - \varphi(t - \tau), \text{total carrier density})$ phase space projection (bottom) displaying similar behaviour to the experimental traces at weak feedback. The black spots indicate the frequencies of both stable and unstable external cavity modes.

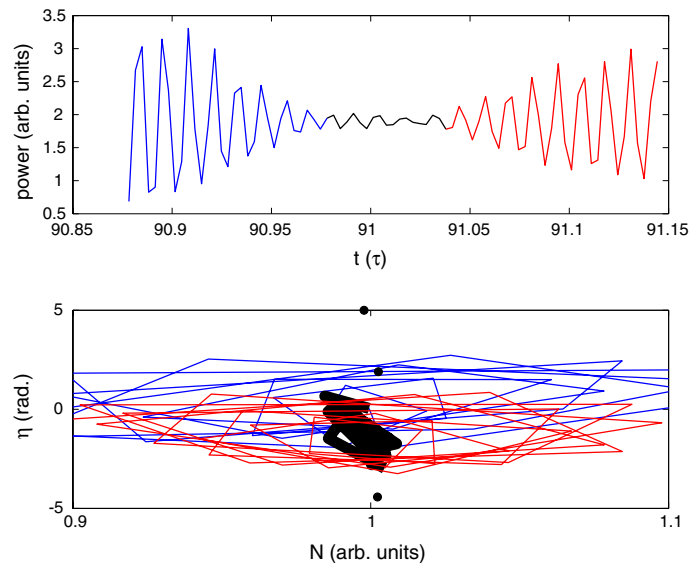


Fig. 9. A second simulated optical power (top) and $(\eta(t), \text{total carrier density})$ phase space projection (bottom) displaying similar behaviour to the experimental traces at weak feedback. The black spots indicate the frequencies of both stable and unstable external cavity modes.

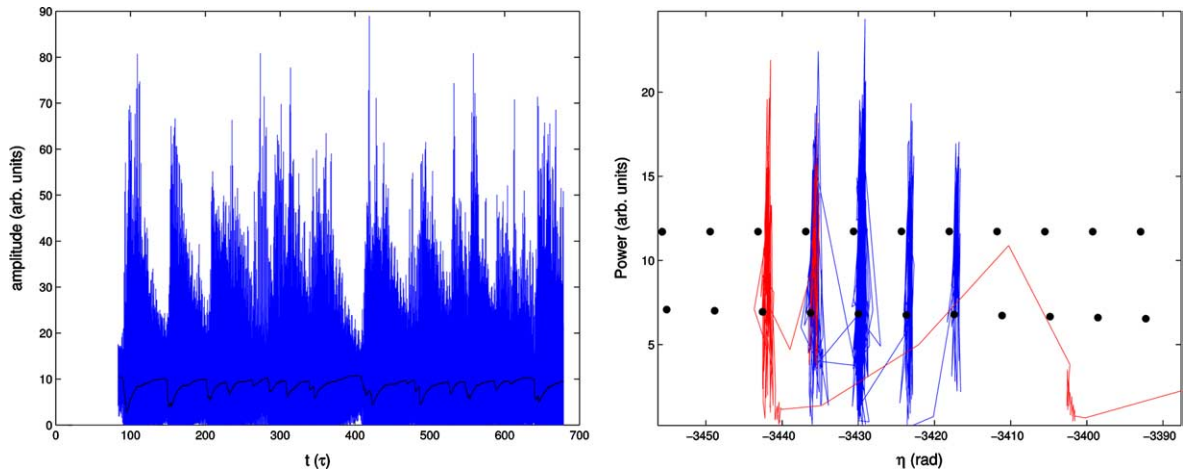


Fig. 10. Simulated instantaneous and time averaged output power (left: blue and black, respectively) and $(\eta(t), \text{output power})$ phase space projection (right). The total power, averaged over the delay time (black) exhibits low frequency power dropouts, similar to those presented in the experimental section. The phase space projection illustrates the case just preceding a power dropout where the lasing frequency hops from external cavity mode to mode before colliding with a saddle point. The black spots indicate the frequencies of both stable (top row) and unstable (bottom row) external cavity modes. (For interpretation of the references to colour in this figure legend, the reader is referred to the web version of this article.)

A is the saturable absorption and β is the ratio of the saturation intensities in the pumped and unpumped regions.

The parameter values are shown on Table 1 and are typical of semiconductor quantum well laser devices. In the following, we choose the bias current so that it corresponds well to the experimental self-pulsing dynamics in the free running regime i.e. the laser's power does not go to zero between laser pulses but instead oscillates about a mean steady state power (see experimental trace on Fig. 2). Some intensity time series of the laser intensity are shown on Figs. 8 and 9 for weak feedback levels. As for the experiment, we observe interruptions of the periodic oscillations over a few periods. In addition, the projection of the trajectory in the η - N plane reveals that oscillations prior to and after the strong reduction of amplitudes are located in different regions of the space indicating that these interruptions can be associated with a transition between two limit cycles. Moreover, the trajectory is near an external cavity mode, which might be stable if the laser was without absorber, when the oscillation is strongly reduced. This behaviour is similar to that reported by Arecchi and

collaborators [19]. On increasing the feedback further, the amplitude variation increases until we reach the case on Fig. 10 where we have reached a LFF regime in the time averaged output.

4. Discussion and conclusions

In the article, we have analysed the dynamics of a self-pulsating semiconductor under the influence of optical feedback. In particular, we observed strong amplitude modulations associated with hopping between limit cycles. As the feedback is further increases, we observed, as for cw lasers, a route to LFFs and coherence collapse. We also note that the threshold for coherence collapse is higher than for cw lasers although the laser intensity remains far from zero between consecutive pulses. To further investigate the behaviour of self-pulsating semiconductor lasers with optical feedback, it would be useful to design two section lasers and analyse the dynamics as the two injection currents are varied. Thus one could compare the case where the laser exhibits pulsing from zero power and compare it with the situation here.

Acknowledgement

This work was supported by Science Foundation Ireland under contract number sfi/01/fi/co. We also gratefully acknowledge Brian Corbett for providing the devices used in this work.

References

- [1] B. Krauskopf, D. Lenstra, *Fundamental Issues of Nonlinear Laser Dynamics*, Melville, New York, AIP, 2000.
- [2] T. Sano, *Phys. Rev. A* 50 (1994) 2719.
- [3] G. van Tartwijk, A. Levine, D. Lenstra, *IEEE Sel. Top. Quantum Electron.* 1 (1995) 466.
- [4] I. Fischer, G.H.M. van Tartwijk, A.M. Levine, W. Elsaesser, E.O. Gobel, D. Lenstra, *Phys. Rev. Lett.* 76 (1996) 220.
- [5] G. Huyet, P.A. Porta, S.P. Hegarty, J.G. McInerney, F. Holland, *Opt. Commun.* 180 (2000) 339.
- [6] C. Harder, K.Y. Lau, A. Yariv, *IEEE J. Quantum Electron.* QE-19 (1982) 1351.
- [7] M. Yamada, *IEEE J. Quantum Electron.* 29 (1993) 1330.
- [8] G.H.M. van Tartwijk, Maxi San Miguel, *IEEE J. Quantum Electron.* QE-32 (1996) 1191.
- [9] Y. Simler, J. Gamelin, S. Wang, *IEEE Photon. Technol. Lett.* 4 (1992) 329.
- [10] T.W. Carr, *Eur. Phys. J. D* 19 (2002) 245.
- [11] R. Lang, K. Kobayashi, *IEEE J. Quantum Electron.* QE-16 (1980) 347.
- [12] T. Yalcinkaya, Y.C. Lai, *Phys. Rev. Lett.* 79 (1997) 3885.
- [13] J. Moerk, B. Tromborg, *IEEE Photon. Technol. Lett.* 2 (1990) 21.
- [14] B. Tromborg, J.H. Osmundsen, H. Olesen, *IEEE J. Quantum Electron.* QE-20 (1984) 1023.
- [15] J. Helms, K. Petermann, *IEEE J. Quantum Electron.* QE-26 (1990) 833.
- [16] A. Ritter, H. Haug, *J. Opt. Soc. Am. B* 10 (1993) 130.
- [17] A. Levine, G. van Tartwijk, D. Lenstra, T. Erneux, *Phys. Rev. A* 52 (1995) R3436.
- [18] G. Lythe, T. Erneux, A. Gavrielides, V. Kovanis, *Phys. Rev. A* 55 (1997) 4443.
- [19] F.T. Arecchi, A. Lapucci, R. Meucci, J.A. Roversi, P.H. Couillet, *Europhys. Lett.* 6 (1988) 677.